Spring 5-2-2021

Effects of Halogen Bonding on 13C NMR Shifts of Various Tolan Species

Anthony Lybrand

Effects of Halogen Bonding on ^{13}C NMR Shifts of Various Tolan Species

By

Anthony Max Lybrand

A thesis submitted to the faculty of The University of Mississippi in partial fulfillment of the requirements of the Sally McDonnell Barksdale Honors College.

Oxford, MS

May 2021

Approved By

Advisor: Professor Daniel Mattern _____

Reader: Professor Davita Watkins _____

Reader: Professor Emily Rowland _____

DEDICATION

This thesis is dedicated to everyone who guided and encouraged me throughout the 2 years that I worked on this project. Thank you.

ACKNOWLEDGEMENTS

I would first and foremost like to thank my research advisor, Dr. Mattern. Dr. Mattern has always been patient with me and has always tried to answer all of my many questions to his fullest ability. I would also like to thank Joshua Peltan for helping me gain some of his astoundingly large amount of practical knowledge in chemistry. Also in my lab group, I would like to specifically thank Nickie Tiwari for helping me keep calm and positive-minded about my work. I also want to thank Cashen Stark in my lab group for offering ideas and assistance in the lab with anything that I might need help with. Lastly, I want to thank all of my friends for making this more enjoyable when the chemistry just did not seem to work.

ABSTRACT

ANTHONY MAX LYBRAND: Effects of Halogen Bonding on ^{13}C NMR Shifts of various Tolan species (Under the direction of Dr. Daniel Mattern)

Halogen bonding is slowly becoming a more and more useful part of the world of chemistry and is beginning to be incorporated into various aspects of the chemical industry. This study's purpose is to determine whether or not halogen bonding can cause any effect in the ^{13}C NMR shifts. The specific purpose of this study is to determine whether these chemical shifts change when a Lewis Base is added to the dissolved sample. In order to do this, the tolan species (4-iodotolan and 4-chlorotolan) had to be synthesized. Once synthesized, the tolan species were analyzed via NMR. NMR data indicated that, although there is some halogen bonding going on, the extent to which it is going on is not known. Similarly, there are many effects and phenomena in play that are simply unknown at this time and need a great deal of study.

PREFACE

This project has had many points where progress was at a screeching halt, however the project has also greatly honed my practical knowledge and also my theoretical knowledge of organic chemistry.

TABLE OF CONTENTS

LIST OF TABLES

LIST OF ABBREVIATIONS

EtSH	Ethanethiol
Py	Pyridine
PPh_3	Triphenylphosphine
4-IT	4-Iodotolan
4-ClT	4-Chlorotolan

LIST OF FIGURES

Chapter 1

Halogen Bonding and the σ Hole Effect

According to the IUPAC definition of a halogen bond, halogen bonding is a form of attractive interaction between the electrophilic region of specific halogen atoms in a molecule and the nucleophilic region of another or the same molecule.[1] Per the definition of a halogen bond, the electrophilic region can be adequately described as a Lewis acid and the nucleophilic region as a Lewis base. More specifically, the Lewis acid is a halogen-bond donor and the Lewis base a halogen-bond acceptor. The optimal Lewis acids are those that are more polarizable, with the exception of fluorine-based Lewis acids due to the high electronegativity of fluorine.[2] Due to this, iodine is usually the ideal halogen to use as the electrophilic region, however chlorine and bromine could also exhibit halogen bonding to a lesser degree. There is not an optimal Lewis base due to the relatively small amount of information regarding halogen bonding; however, according to the IUPAC definition of a halogen bond, a lone-pair-possessing atom, a π system, or an anion all can function as the Lewis base for a halogen bond.[1,2] In previous studies, pyridine, triphenylphosphine, and 3-propanethiol were used as Lewis bases for the studying of halogen bonding and how the NMR shifts of a molecule are affected by halogen bonding.[3]

In the Lewis acid, next to the halogen atom away from the rest of the Lewis acid,

there is a small region of very low electrostatic potential that allows for the halogen atom to operate as a Lewis acid. This small region, shown below,[2] is called a "σ hole" and is ultimately what allows halogen bonding to exist.[2] The Lewis base, by definition, is a lone pair donor and has a region of very high electrostatic potential that allows for a bond similar to that of a hydrogen bond to form between the Lewis base and the σ hole of the Lewis acid.

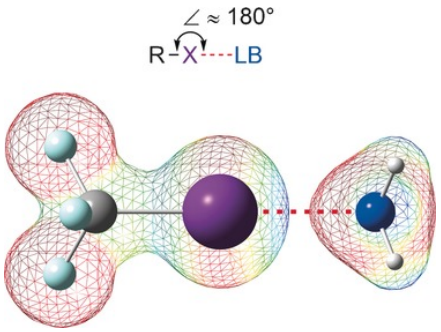

Figure 1.1: Halogen bonding and the σ Hole Effect.

Chapter 2

NMR Background

In order to observe halogen bonding, an iodine was placed on a tolan skeleton (shown below). As previously mentioned, iodine allows for the highest degree of halogen bonding to take place. Although originally there is electron density on and around the Lewis acid and Lewis base, a portion of this electron density is inserted into the R-X bond. Based on the idea that some of the electron density is moved, in theory, a change in ^{13}C NMR chemical shifts should be observed in carbons close to the halogen. By looking at the ^{13}C NMR shifts of each spectrum, it could be possible to quantify the strength of the halogen bonding. Based on previous research,[4] it has been shown that substituents in the 1 position in tolan can influence the chemical shifts of carbons on the alkyne bridge and through to the distant benzene ring of the tolan. Of interest in particular is how far the effect of halogen bonding travels throughout the tolan. As a control, chlorine was used since they are not subject to the effects of halogen bonding like iodine is.

In order to test how the NMR shifts of the tolan were affected by the addition of a Lewis base, a reference spectrum for the tolan will be taken with roughly 15 mg of 4-iodotolan in 0.8 mL of $CDCl_3$. Then the representative halogen-bond acceptors (Lewis

bases) will be added in amounts starting at roughly 1 molar equivalent. The halogen-bond acceptors will be pyridine, triphenylphosphine, and ethanethiol. At specific ratios, the NMR spectrum will be taken and the chemical shifts of each carbon will be noted and compared to the reference spectrum to see how the chemical shift changed due to the addition of the halogen-bond acceptor. This is done until a predetermined ratio is achieved.

Before analyzing each spectrum individually, it is important to note that some carbons are more prone to the effect than others due to resonance and induction effects. This is denoted by a rho value that is a measure of the induction and resonance parameters, based on a Hammett plot analysis of seven substituents.[4] The carbons most affected by the substituent, in this case an iodine, in terms of resonance are C2 and C4 which are in the ortho and para positions on the substituted ring. The induction effect does not provide as significant an effect as resonance; however C1, C4, and C6 appear to offer the highest rho values for the induction parameter.[4] Specifically, C4 should change the most based on the rho values for the induction and resonance parameters and should be taken special note of in the ^{13}C NMR.

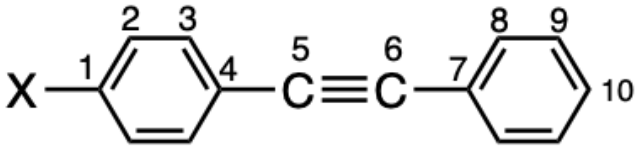

Figure 2.1: Tolan Carbon assignments.

Chapter 3

Analysis of NMR Spectra

3.1 Procedure

To an NMR tube was added the tolan (0.0493 mmol) and 0.8 mL of $CDCl_3$, making a 0.616 M solution. Each sample was first analyzed by 256 scan ^{13}C NMR in order to get a baseline NMR to compare to each addition of base. In the first sample, a 1 mol equivalent of EtSH (1:1 ratio) was added and another 256 scan ^{13}C NMR was taken. This was repeated for ratios of 5:1, 10:1, 20:1, and 40:1. The procedure was then repeated with a fresh sample of the tolan species, with pyridine and PPh_3 added instead. The PPh_3 was added in ratios of 1:1, 2:1, 5:1, 10:1, and 20:1 in order to prevent issues with dissolving the Lewis base due to its increased mass relative to the other Lewis bases.. Each NMR was analyzed and the data compiled and compared.

3.2 Analysis

For each NMR, the chemical shifts of the tolan were recorded and compared to the chemical shifts of the pure tolan species. All shifts are measured in ppm and all spectra are referenced to the TMS peak at 0 ppm. The peaks are labeled relative to their

position to the C-X bond. All data can be found in the tables below.

Analysis of the data indicates that addition of a halogen-bond acceptor does have a systemwide effect on the chemical shifts of the various tolan species;, however, of important note are the chemical shift changes at C1. The shift changes at C1 specifically for 4-iodotolan (4-IT) are large in magnitude and positive (deshielded) for all halogen-bond acceptors, which does indicate that the halogen-bond acceptors are interacting with the iodine, the halogen-bond donor. Further evidence can be found in the corresponding C1 shift changes for 4-chlorotolan (4-ClT) and unsubstituted tolan. In these compounds, the chemical shift change is either effectively 0 (EtSH), not significant (Py), or larger in magnitude and negative (PPh_3) relative to the 4-IT shift changes on C1.

Comparison of the various additions of Lewis bases does not appear to follow any sort of general trend among the 3 Lewis bases. Addition of EtSH results in an almost uniformly small, positive shift change throughout the entire system with the exception of C1. Addition of Py appears to have no preference for being positive or negative; however, C5 and C6 appear to have a significant positive shift change through all halogen-bond donors. Addition of PPh_3 results in an overwhelmingly negative shift change with the exceptions being C1 on 4-IT and C5 and C6 not showing any significant change from the reference peaks.

In terms of what is expected from the rho values detailed earlier, the data for C2, C4, and C6 do not appear to show any significant difference between a halogen-bond donor like 4-IT and a “normal” compound such as 4-ClT or tolan. The lack of any

significant amount of positive shift changes at C2, C4, and C6 for all 3 tolan species indicates that neither resonance nor induction is the phenomenon that is occurring. The reason for this is currently unknown.

Of interest are the shift changes for addition of PPh_3 to 4-ClT. Looking at the final shift changes, there does not appear to be anything significant happening to C10 and it is even smaller in magnitude than the shift changes for addition of PPh_3 to 4-IT and tolan. However, analysis of the individual shift changes after each addition of Lewis base indicates that there is a relatively large negative shift change at 1:1 and a much larger positive shift change at 2:1 that then quickly shifts to a relatively normal downward-trending slope. The reason for this is not currently known and it is unclear why PPh_3 and 4-ClT alone exhibit this and not 4-IT, tolan, and Py.

Finally, the trendlines for the data appear to not be uniform. In the case of EtSH, the trendline for the shift changes appears to follow a very normal linear fit. However this is not the case for the Py and PPh_3 NMR trends. In the Py and PPh_3 NMR trends for all tolan species, the data appears to much more closely resemble that of a 2nd-degree polynomial fit with high R^2 values with the only exception being the aforementioned C10 on 4-ClT with addition of PPh_3. The reason for this is unknown at this time but it is likely that there are other factors at play, as evidenced by the use of a 2nd-degree polynomial rather than a linear fit. The linear slopes of all tolans and Lewis bases are shown below as well as the R^2 values for Py and PPh_3 with a linear and a polynomial fit.

EtSH	**C1**	**C2**	**C3**	**C4**	**C5**
4IT	0.093 ± 0.003	0.023 ± 0.002	0.013 ± 0.002	0.036 ± 0.002	0.014 ± 0.001
4ClT	0.002 ± 0.002	0.015 ± 0	0.019 ± 0.001	0.055 ± 0	0.005 ± 0
Tolan	0.012 ± 0.001	0.017 ± 0.001	-0.003 ± 0.003	0.034 ± 0.004	0.023 ± 0
Py	**C1**	**C2**	**C3**	**C4**	**C5**
4IT	0.088 ± 0.023	-0.004 ± 0.005	-0.025 ± 0.002	-0.017 ± 0.011	0.056 ± 0.023
4ClT	-0.04 ± 0.002	-0.004 ± 0.002	0.005 ± 0.002	0.014 ± 0.006	0.042 ± 0.003
Tolan	0.04 ± 0.006	0.033 ± 0.003	-0.029 ± 0.002	-0.02 ± 0.005	0.083 ± 0
PPh_3	**C1**	**C2**	**C3**	**C4**	**C5**
4IT	0.087 ± 0.006	-0.134 ± 0.004	-0.129 ± 0.004	-0.163 ± 0.001	0.005 ± 0.003
4ClT	-0.135 ± 0.007	-0.1 ± 0.007	-0.111 ± 0.006	-0.125 ± 0.007	-0.011 ± 0.001
Tolan	-0.111 ± 0.003	-0.102 ± 0.001	-0.114 ± 0.002	-0.112 ± 0.004	0.001 ± 0

Table 3.1: Shift change in ppm compared to reference ppm values for Carbons 1-5. The uncertainty is the range of the two trials.

EtSH	**C6**	**C7**	**C8**	**C9**	**C10**
4IT	0.041 ± 0	0.036 ± 0.002	0.006 ± 0	0.019 ± 0.002	0.018 ± 0.003
4ClT	0.047 ± 0	0.031 ± 0.001	0.009 ± 0.003	0.019 ± 0.001	0.017 ± 0.001
Tolan	0.023 ± 0	0.034 ± 0.004	-0.003 ± 0.003	0.017 ± 0.001	0.012 ± 0.001
Py	**C6**	**C7**	**C8**	**C9**	**C10**
4IT	0.087 ± 0.026	-0.009 ± 0.004	-0.021 ± 0.001	0.02 ± 0.007	0.024 ± 0.004
4ClT	0.109 ± 0.002	-0.019 ± 0.008	-0.018 ± 0.001	0.028 ± 0.003	0.038 ± 0.004
Tolan	0.083 ± 0	-0.02 ± 0.005	-0.029 ± 0.002	0.033 ± 0.003	0.04 ± 0.006
PPh_3	**C6**	**C7**	**C8**	**C9**	**C10**
4IT	-0.002 ± 0.006	-0.11 ± 0.003	-0.118 ± 0.004	-0.099 ± 0.001	-0.095 ± 0.003
4ClT	0.015 ± 0.001	-0.114 ± 0.006	-0.113 ± 0.004	-0.112 ± 0.028	-0.054 ± 0.002
Tolan	0.001 ± 0	-0.112 ± 0.004	-0.114 ± 0.002	-0.102 ± 0.001	-0.111 ± 0.003

Table 3.2: Shift change in ppm compared to reference ppm values for Carbons 6-10. The uncertainty is the range of the two trials.

Δ ppm (from previous)	**C10**
1:1	-0.022 ± 0.031
2:1	0.049 ± 0.029
5:1	-0.016 ± 0.001
10:1	-0.025 ± 0.002
20:1	-0.04 ± 0.001

Table 3.3: Shift change in ppm compared to the previous ratio's ppm values for C10 on 4-ClT with PPh_3 as the Lewis base. The uncertainty is the range of the two trials.

Py	**C1**	**C2**	**C3**	**C4**	**C5**	**C6**	**C7**	**C8**	**C9**	**C10**	***Average***
4IT	0.995	0.298	0.969	0.881	0.983	0.999	0.465	0.946	0.975	0.998	0.851
4ClT	0.970	0.362	0.645	0.961	0.958	0.983	0.907	0.950	0.980	0.986	0.870
Tolan	0.995	0.990	0.955	0.920	0.997	0.997	0.920	0.955	0.990	0.995	0.971
PPh_3	**C1**	**C2**	**C3**	**C4**	**C5**	**C6**	**C7**	**C8**	**C9**	**C10**	***Average***
4IT	0.999	0.993	0.994	0.995	0.669	0.350	0.992	0.992	0.989	0.991	0.896
4ClT	0.996	0.997	0.995	0.940	0.875	0.985	0.993	0.995	0.966	0.559	0.930
Tolan	0.993	0.992	0.993	0.993	0.122	0.122	0.993	0.993	0.992	0.993	0.819

Table 3.4: R^2 values for Py and PPh_3 using a linear fit trendline.

Py	**C1**	**C2**	**C3**	**C4**	**C5**	**C6**	**C7**	**C8**	**C9**	**C10**	***Average***
4IT	0.999	0.994	0.996	0.989	0.998	0.999	0.970	0.998	1.000	0.999	0.994
4ClT	0.976	0.858	0.976	0.995	0.989	0.984	0.972	0.968	0.993	0.992	0.970
Tolan	0.997	0.998	0.995	0.993	0.998	0.998	0.993	0.995	0.998	0.997	0.996
PPh_3	**C1**	**C2**	**C3**	**C4**	**C5**	**C6**	**C7**	**C8**	**C9**	**C10**	***Average***
4IT	0.999	1.000	1.000	1.000	0.952	0.771	0.999	1.000	1.000	0.998	0.972
4ClT	1.000	0.997	1.000	1.000	0.996	0.990	1.000	1.000	1.000	0.677	0.966
Tolan	1.000	0.999	1.000	1.000	0.882	0.882	1.000	1.000	0.999	1.000	0.976

Table 3.5: R^2 values for Py and PPh_3 using a 2nd-degree polynomial fit.

EtSH	**C1**	**C2**	**C3**	**C4**	**C5**	**C6**	**C7**	**C8**	**C9**	**C10**
4IT	0.002230	0.000568	0.000326	0.000885	0.000357	0.000982	0.000873	0.000164	0.000481	0.000445
4ClT	0.000053	0.000408	0.000502	0.001380	0.000128	0.001180	0.000798	0.000201	0.000483	0.000465
Tolan	0.000331	0.000438	-0.000068	0.000878	0.000589	0.000589	0.000878	-0.000068	0.000438	0.000331
Py	**C1**	**C2**	**C3**	**C4**	**C5**	**C6**	**C7**	**C8**	**C9**	**C10**
4IT	0.002240	-0.000103	-0.000633	-0.000442	0.001420	0.002220	-0.000205	-0.000514	0.000501	0.000602
4ClT	-0.001020	-0.000091	0.000139	0.000358	0.001080	0.002820	-0.000504	-0.000472	0.000720	0.000965
Tolan	0.001040	0.000849	-0.000731	-0.000499	0.002130	0.002130	-0.000499	-0.000731	0.000849	0.001040
PPh3	**C1**	**C2**	**C3**	**C4**	**C5**	**C6**	**C7**	**C8**	**C9**	**C10**
4IT	0.004260	-0.006690	-0.006430	-0.008060	0.000260	-0.000107	-0.005410	-0.005870	-0.004900	-0.004640
4ClT	-0.006740	-0.005180	-0.005530	-0.006280	-0.000558	0.000774	-0.005710	-0.005680	-0.003990	-0.002780
Tolan	-0.005540	-0.005070	-0.005690	-0.005580	0.000075	0.000075	-0.005580	-0.005690	-0.005070	-0.005540

Table 3.6: Slopes for the linear trendlines of each analyzed sample.

Chapter 4

Synthetic Procedures

4.1 Synthesis of 4-Iodotolan

Phenylacetylene (0.75 mL, 6.85 mmol) was added to a degassed suspension of 4-iodoaniline (1000 mg, 4.56 mmol), $PdCl_2(PPh_3)_2$ (48 mg, 0.069 mmol), and CuI (13.5 mg, 0.069 mmol) in a mixture 3/1 of Et_3N/THF (12 mL). The reaction was stirred for 2 h under nitrogen atmosphere at room temperature. The mixture was then diluted with EtOAc, washed with aqueous NH_4Cl, dried over anhydrous Na_2SO_4 and the solvent was removed under reduced pressure. The residue was purified by column chromatography (EtOAc/hexane: 2/8) to give 4-aminotolan and was confirmed by NMR.

The amine was suspended in distilled water, a solution of sulfuric acid 98% (0.8 mL) was added and the mixture was cooled to 0°C. Sodium nitrite in water was added dropwise with stirring, keeping the temperature 0–5 °C, over the course of 30 minutes. THF (4 mL) was added to the reaction mixture and then, a solution of potassium iodide (1.286 g, 7.740 mmol) in water (8 mL) was added slowly over the course of 30 minutes. After 3 hours the reaction mixture was diluted with EtOAc and washed with saturated Na_2SO_3 solution and brine, dried over anhydrous Na_2SO_4 and concentrated under reduced pressure. The residue was purified by column chromatography (EtOAc/hexane: 1/9) to

give the product as a white solid that showed NMR spectra identical to reported data.[5]

4.2 Synthesis of 4-Chlorotolan

To a round-bottom flask was added $PdCl_2(PPh_3)_2$ (26.6 mg, 0.038 mmol) and CuI (13.6 mg, 0.071 mmol) as well as 1-chloro-4-iodobenzene (428.7 mg, 1.80 mmol). CH_3CN (5 mL) and Et_3N (5 mL) were added in order to form a heterogeneous mixture. The reaction mixture was then degassed by passing a steady stream of N_2 through the mixture for 30 minutes. Phenylacetylene (0.22 mL, 2.0 mmol) was added to the mixture and the mixture was allowed to stir overnight under a nitrogen atmosphere. Once the reaction was complete, the mixture was diluted with aqueous NH_4Cl. The mixture was then extracted with EtOAc and the organic layer washed with brine. The solution was then dried over anhydrous Na_2SO_4 and concentrated under reduced pressure. The product was purified by column chromatography with the elution solvent being 5% EtOAc-hexanes. The product was confirmed by NMR literature values.[6]

Some byproducts of the Sonogashira coupling reaction were created in this synthesis, however none of the byproducts appeared to be in any significant concentrations according to NMR analysis. The only known byproduct is shown below.

Figure 4.1: Byproduct 1,4-diphenylbutadiyne.

Chapter 5

Synthetic Troubles

5.1 4-Iodotolan Unexpected Byproducts

During the synthesis of 4-iodotolan, an unexpected byproduct of the alkyne of 4-aminotolan with water was created that transformed the internal alkyne into a ketone. The ketone was formed by hydration of the internal alkyne with water. This reaction usually requires the use of a mercury catalyst, however this was not required for this reaction to occur. Instead of a diazonium salt forming and nothing happening to the alkyne, the diazonium salt was not forming in a significant capacity and the alkyne was being transformed into a ketone. This is possibly due to the amino group stabilizing the carbocation intermediate that would otherwise be too unstable to form. NMR values calculated via ChemDraw agree with the signals found.

During the next synthesis of 4-iodotolan (same procedure), a byproduct believed to be obtained from impure THF was obtained. The byproduct created was 2-propoxytetrahydrofuran. The impurity was verified by calculated NMR values according to ChemDraw. The mechanism/reaction of the formation of the product is unknown but no chemicals that could supply a propoxy group were used, so it is believed to be an impurity from the THF.

5.2 4-Iodotolan Failed Synthesis

Originally, a 1-step Sonogashira coupling reaction using phenylacetylene and 1,4-diiodobenzene was utilized. This reaction was ultimately not used due to the inability to separate 1,4-diiodobenzene from the 4-IT due to the many similar properties that the two compounds share and instead the diazonium salt synthesis was used to combat this issue.

Chapter 6

Peak Assignments

6.1 4-Iodotolan

C4, C7, C9, and C10 on 4-IT were not able to be differentiated strictly by the analysis of one-dimensional NMR spectra. In order to assign the peaks for each carbon, a COSY, HMBC, and HMQC spectrum were taken.

H2 at 7.68 ppm was 2-bond coupled to C4, establishing the C4 chemical shift as 122.8 ppm. This automatically gives 122.9 ppm to be C7 due to the extremely similar chemical environments of the carbons.

C9 and C10 were differentiated due to their different peak heights as the peak at 128.3 ppm had double the height of the peak at 128.5 ppm, which signified that it corresponded to 2 equivalent carbons. The 128.5 ppm peak was also 3-bond coupled to H3 and the 128.3 ppm peak directly bonded to H4. This means that C9 and C10 must be 128.3 ppm and 128.5 ppm, respectively.

6.2 4-Chlorotolan

C2, C4, C7, C9, and C10 were unable to be resolved strictly by the analysis of one-dimensional NMR spectra. In order to assign these peaks, a COSY, HMBC, and

HMQC spectrum were taken.

H2 at 7.48 ppm was 2-bond coupled to 121.8 ppm which corresponds to C4. This means that C7 must be 122.9 ppm and this is confirmed by H3 at 7.56 ppm 2-bond coupling with the peak at 122.9 ppm.

H3 was 3-bond coupled to the 128.5 ppm peak. This means that C10 corresponds to the 128.5 ppm peak. H1 at 7.48 ppm was HMQC coupled to the 128.7 ppm peak which must correspond to C2. This leaves C9 as 128.4.

Chapter 7

Future Work

The analysis of the various tolan species answered fewer questions than it created. In order to answer some of these questions, such as whether the trends for 4-ClT and 4-IT can be connected to other halogens, much more work could be done. Specifically, it would be greatly beneficial to employ the use of all halogenated tolans and compare the effects to what has already been observed in this study. Other useful work could include using similarly structured bases (such as all ethyl-based compounds or all aromatic species), testing for an upper limit on the effect of the Lewis base on the Lewis acid by using an extreme excess of Lewis base, and using molar ratios close to 2:1 for testing of PPh_3 on C10 of 4-ClT. Beyond this, there are still many studies that could be done to help answer some of the questions and research presented in this study.

Conclusions

Overall, the work of this study left many things unanswered and brought about even more unanswered questions. However, this study does show that, while the extent of the effect is not yet known, there is a noticeable halogen-bonding effect and that there is a significant amount of work that can be done to further understand the phenomena that is occurring.

Bibliography

1. Desiraju, G; Ho, P; Kloo, L; Legon, A; Marquardt, R; Metrangolo, P; Politzer, P; Resnati, G; Rissanen, K. Definition of the halogen bond (IUPAC Recommendations 2013). *Pure Appl. Chem.* **2013**, Vol. 85, No. 8, pp. 1711–1713.

2. Bulfield, D; Huber, S. Halogen Bonding in Organic Synthesis and Organocatalysis. *Chem. Eur. J.* **2016**, 22, 14434 – 14450

3. Long, James, "Effects of Halogen Bonding on 13C NMR Shifts of Iodotolan" (2019). Honors Theses. 1100. https://egrove.olemiss.edu/hon_thesis/1100/

4. Crumpler, Reece, "13C NMR Substituent Effects on para-Substituted Tolans: Using Deuteration to Assign 13C Signals in Methyltolan" (2020). Honors Theses. 1342. https://egrove.olemiss.edu/hon_thesis/1342

5. Márquez, I. R.; Fuentes, N.; Cruz, C. M.; Puente-Muñoz, V.; Sotorrios, L.; Marcos, M. L.; Choquesillo-Lazarte, D.; Biel, B.; Crovetto, L.; Gómez-Bengoa, E.; González, M. T.; Martin, R.; Cuerva, J. M.; Campaña, A. G. Versatile Synthesis and Enlargement of Functionalized Distorted Heptagon-Containing Nanographenes. Chemical Science 2017, 8 (2), 1068–1074.

6. Ruengsangtongkul, S.; Chaisan, N.; Thongsornkleeb, C.; Tummatorn, J.; Ruchirawat, S. Rate Enhancement in CAN-Promoted Pd(PPh3)2Cl2-Catalyzed Oxidative Cyclization: Synthesis of 2-Ketofuran-4-Carboxylate Esters. Organic Letters 2019, 21 (8), 2514–2517.

7. Fang, J.-K.; An, D.-L.; Wakamatsu, K.; Ishikawa, T.; Iwanaga, T.; Toyota, S.; Matsuo, D.; Orita, A.; Otera, J. Synthesis and spectroscopic study of diphenylamino-substituted phenylene-(poly)ethynylenes: remarkable effect of acetylenic conjugation modes. https://www.sciencedirect.com/science/article/abs/pii/S0040403909022990 (accessed Apr 22, 2021).

Appendix

Some but not all spectra are included. All spectra are zoomed in from 85 ppm to 140 ppm in order to show only the tolan peaks.

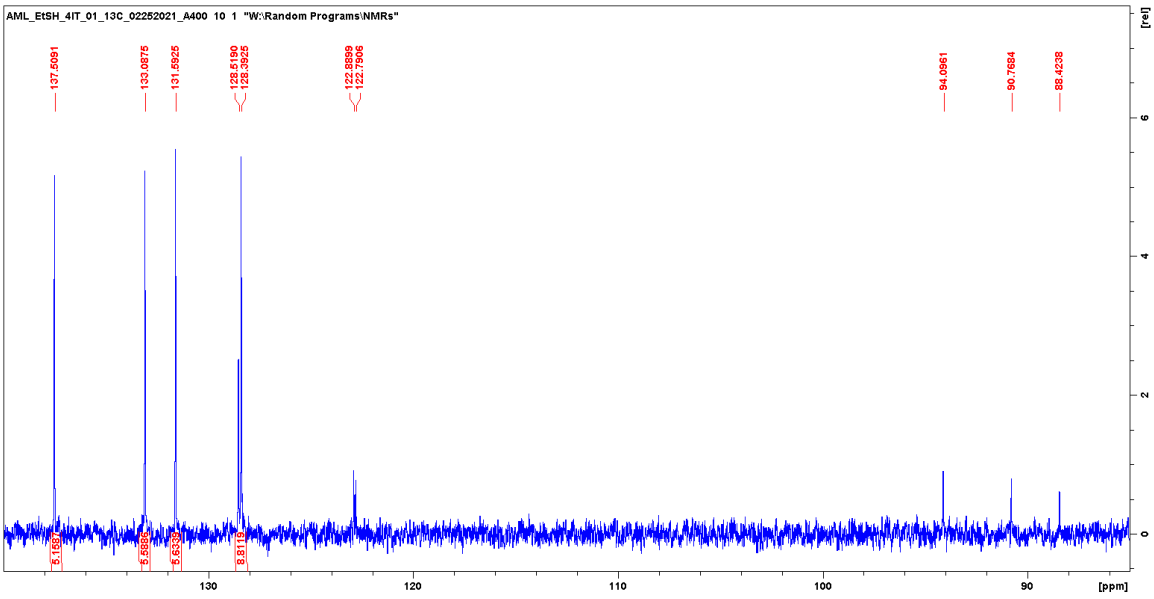

Figure 9.1: 4-IT reference peaks.

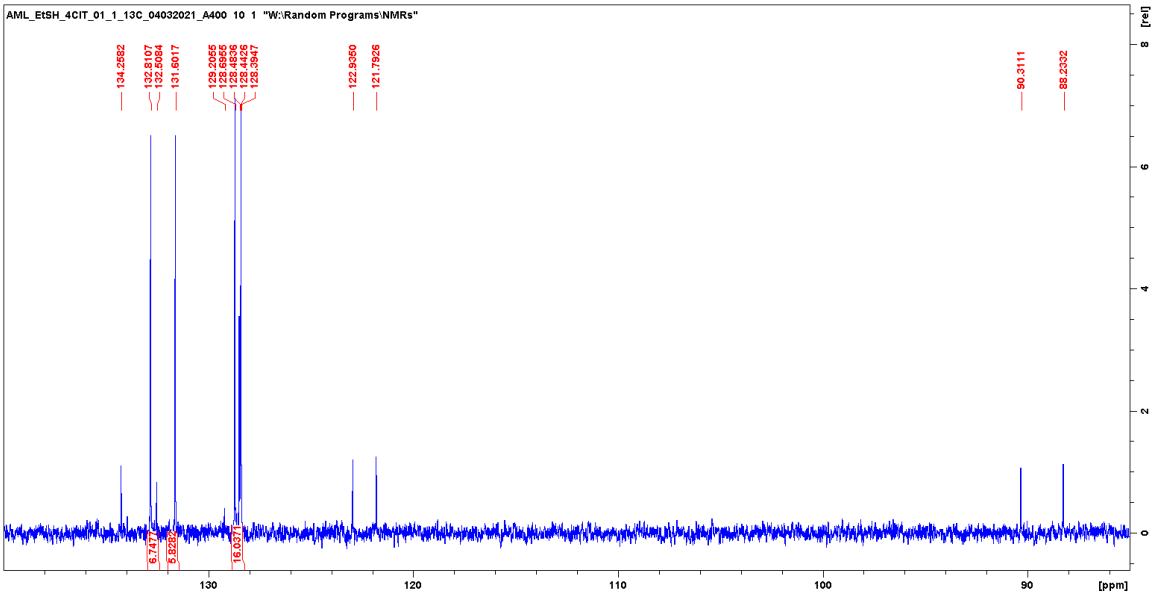

Figure 9.2: 4-ClT reference peaks.

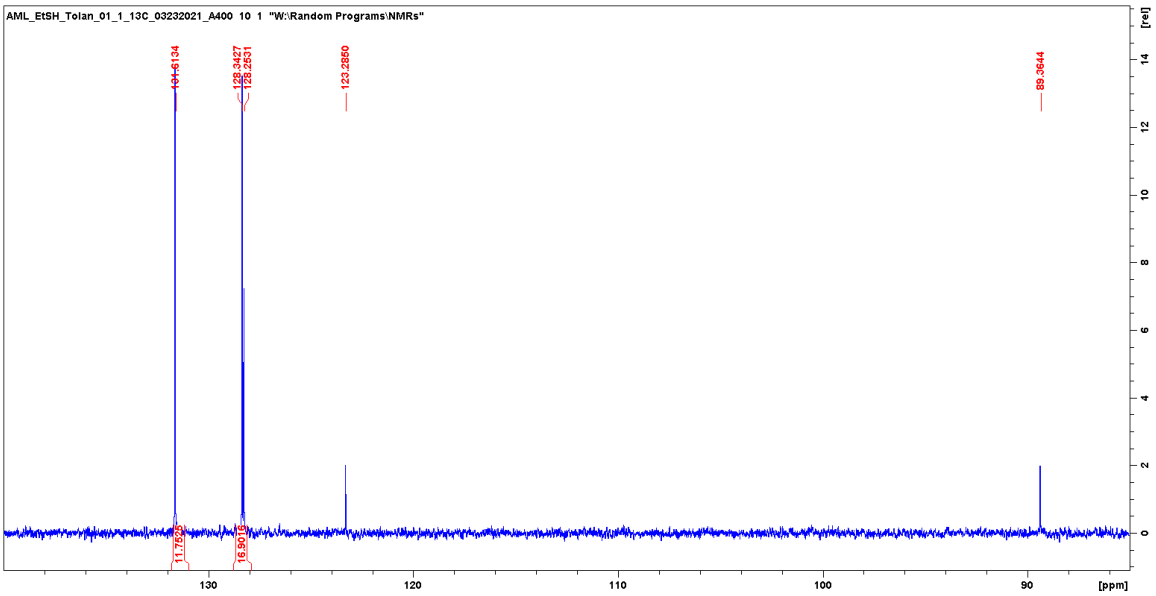

Figure 9.3: Unsubstituted tolan reference peaks.

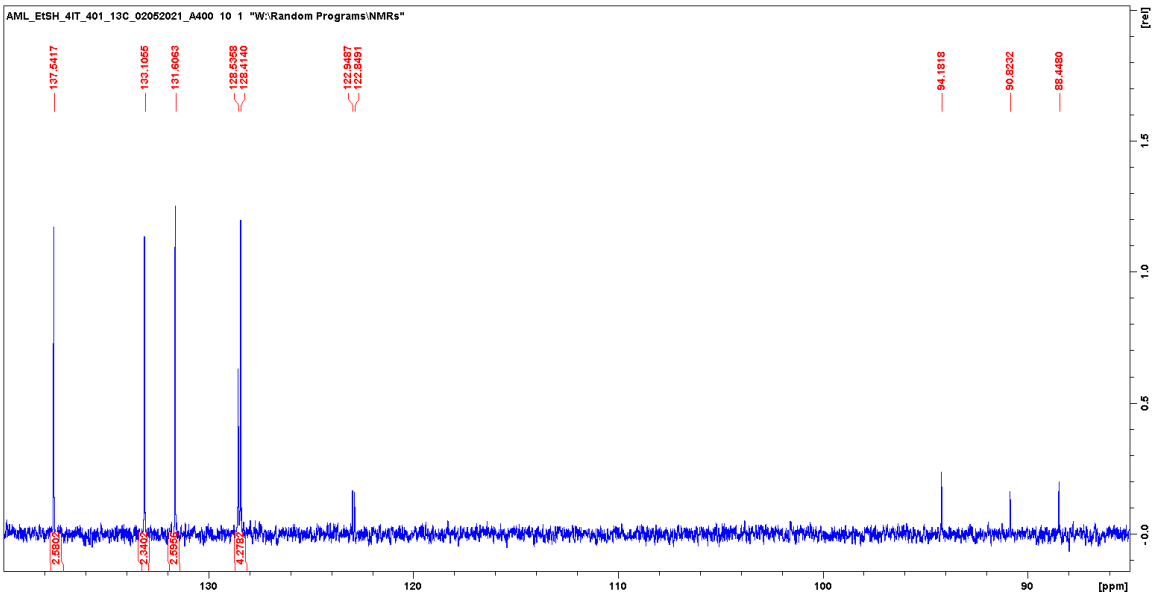

Figure 9.4: 40:1 EtSH:4-IT trial 1 spectrum.

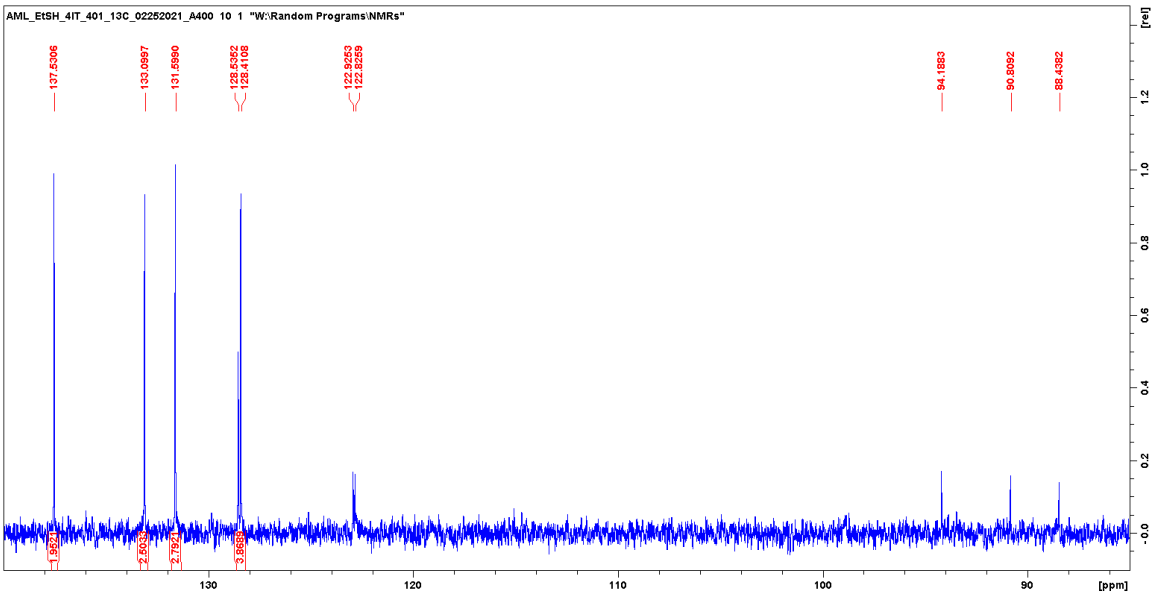

Figure 9.5: 40:1 EtSH:4-IT trial 2 spectrum.

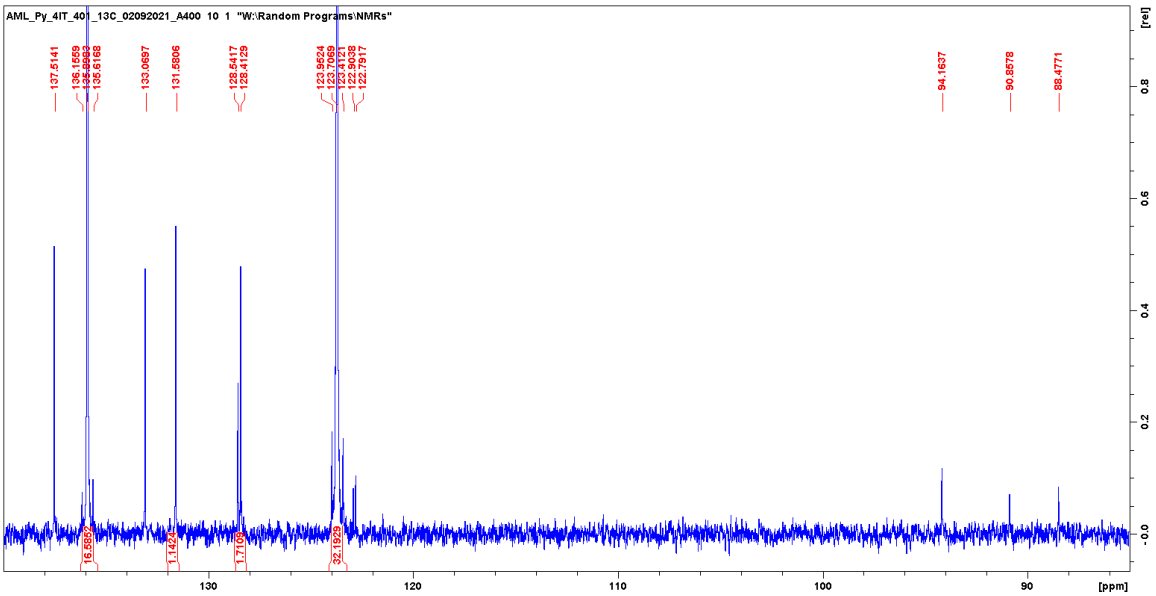

Figure 9.6: 40:1 Py:4-IT trial 1 spectrum.

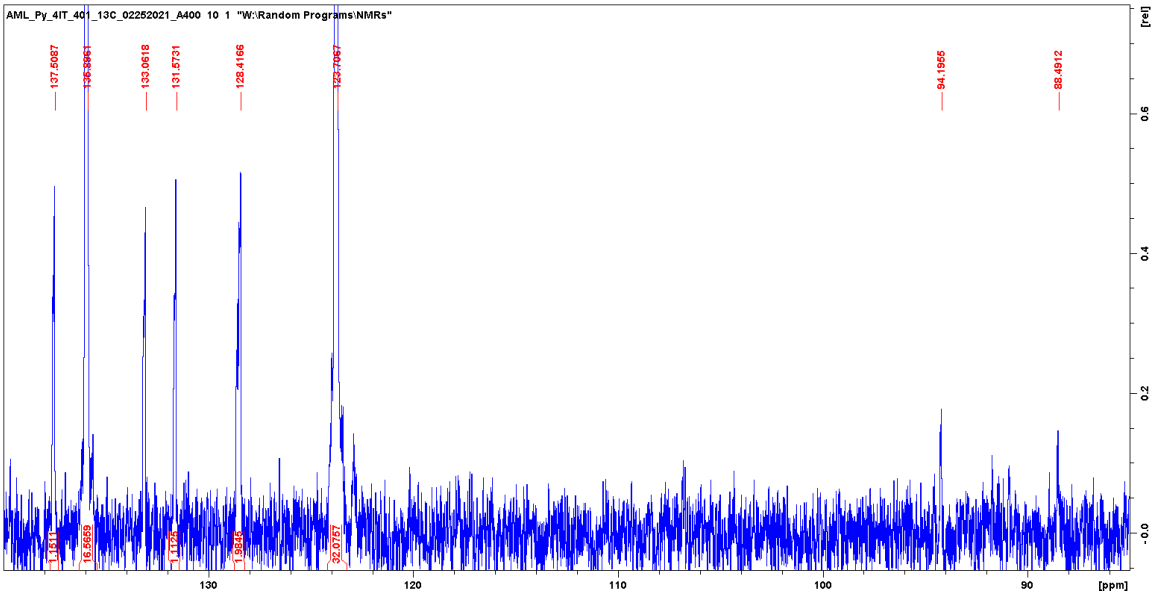

Figure 9.7: 40:1 Py:4-IT trial 2 spectrum.

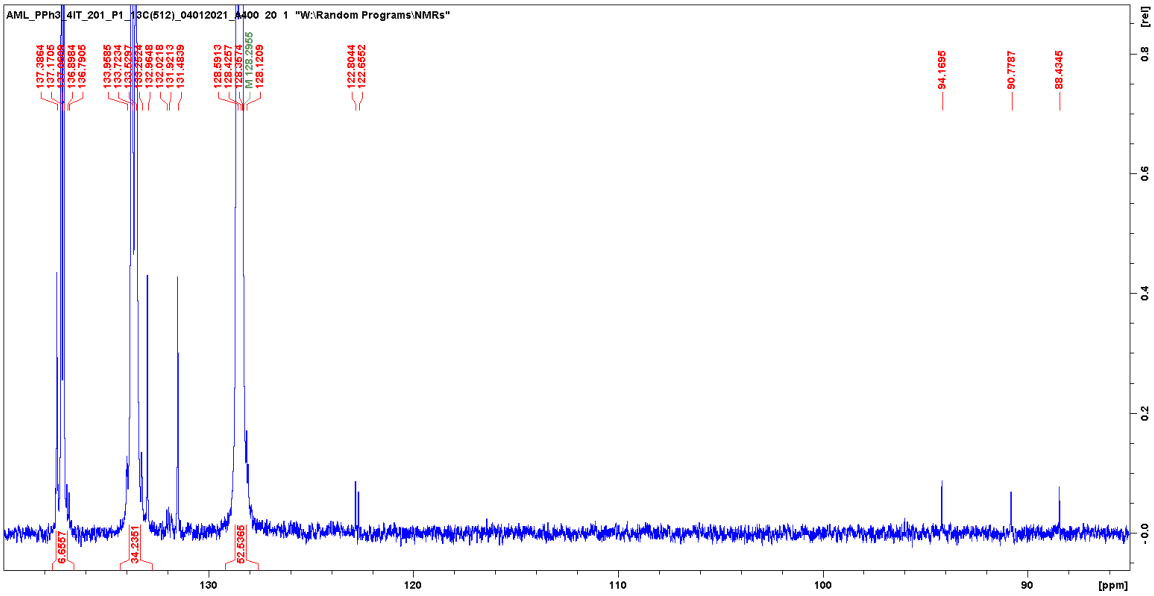

Figure 9.8: 20:1 PPh_3:4-IT trial 1 spectrum.

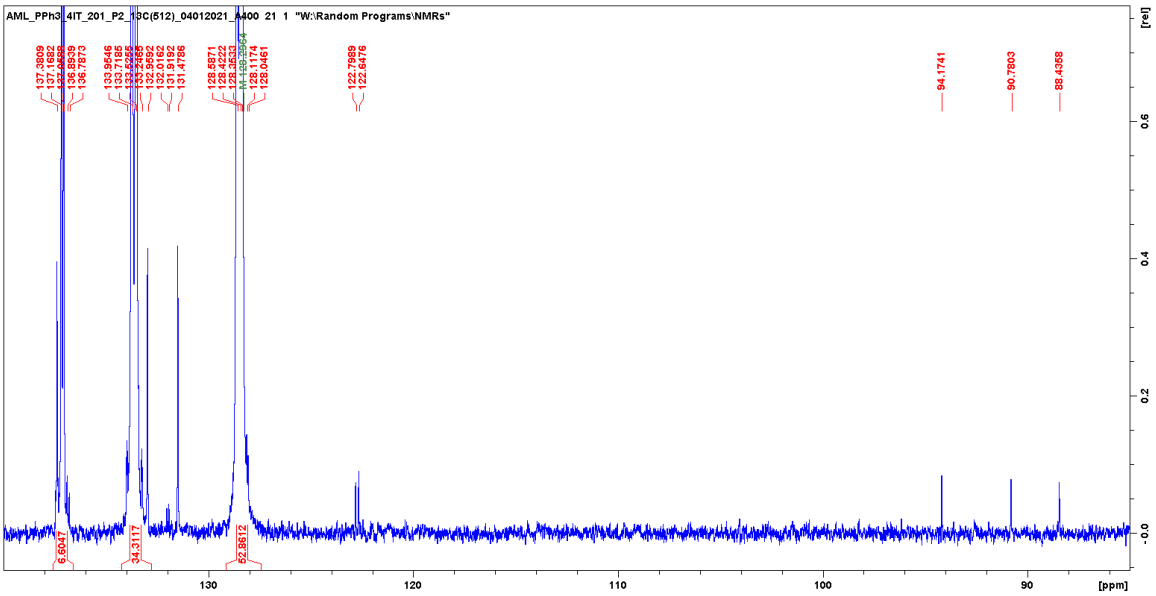

Figure 9.9: 20:1 PPh_3:4-IT trial 2 spectrum.

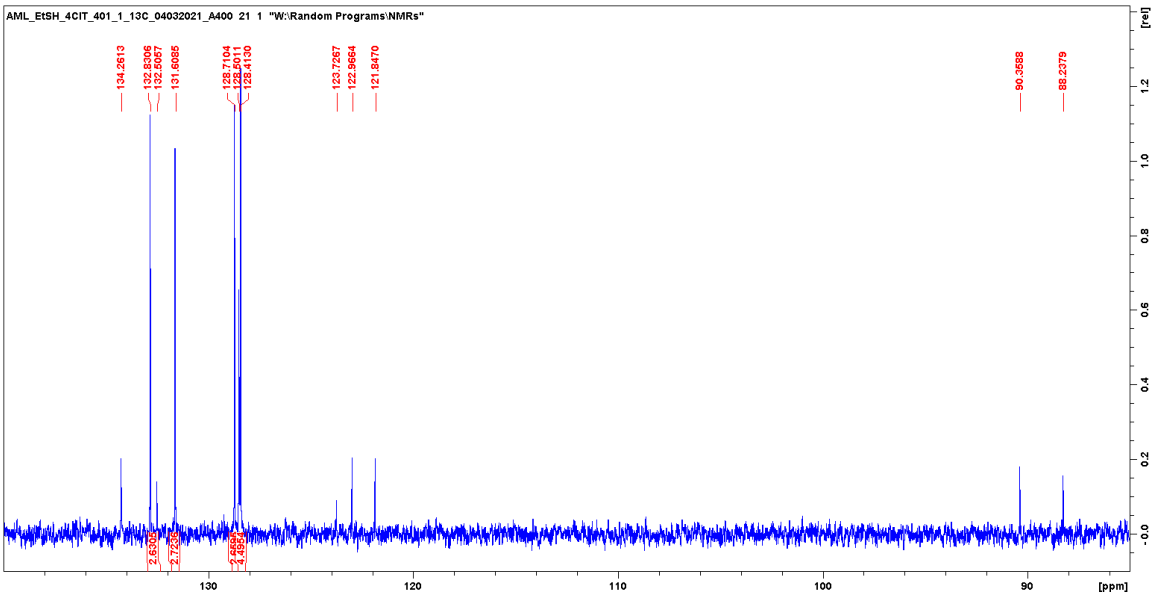

Figure 9.10: 40:1 EtSH:4-ClT trial 1 spectrum.

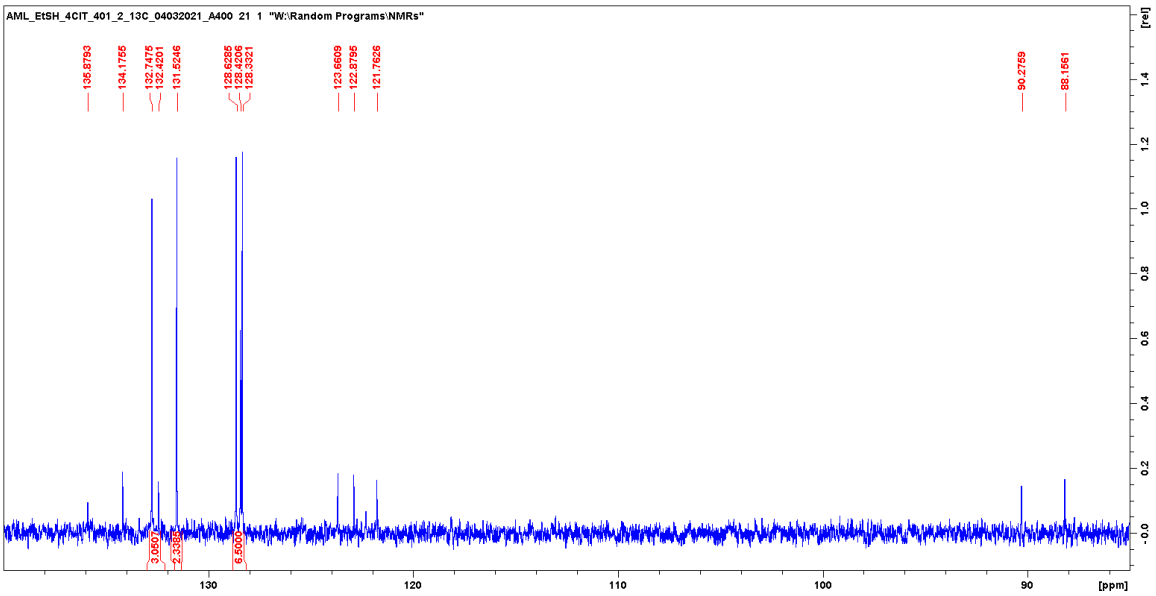

Figure 9.11: 40:1 EtSH:4-ClT trial 2 spectrum.

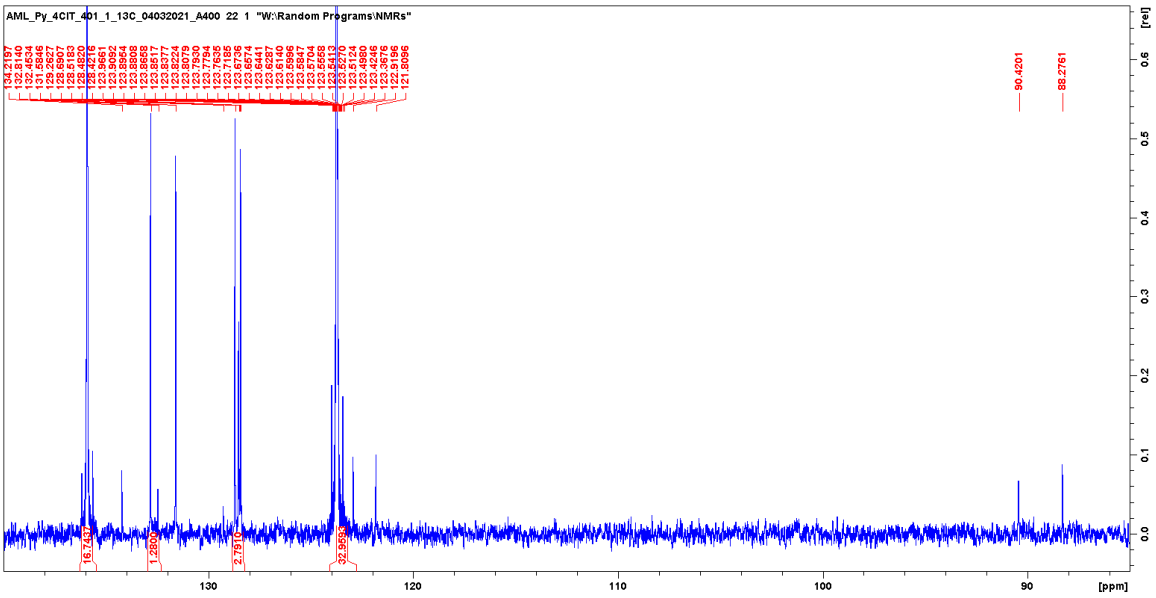

Figure 9.12: 40:1 Py:4-ClT trial 1 spectrum.

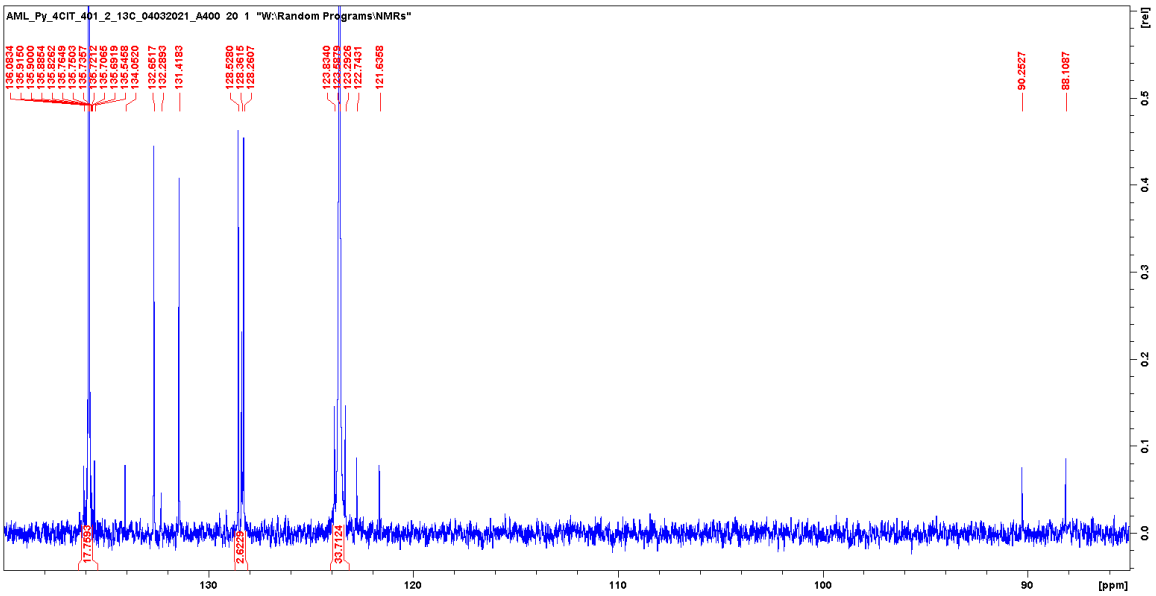

Figure 9.13: 40:1 Py:4-ClT trial 2 spectrum.

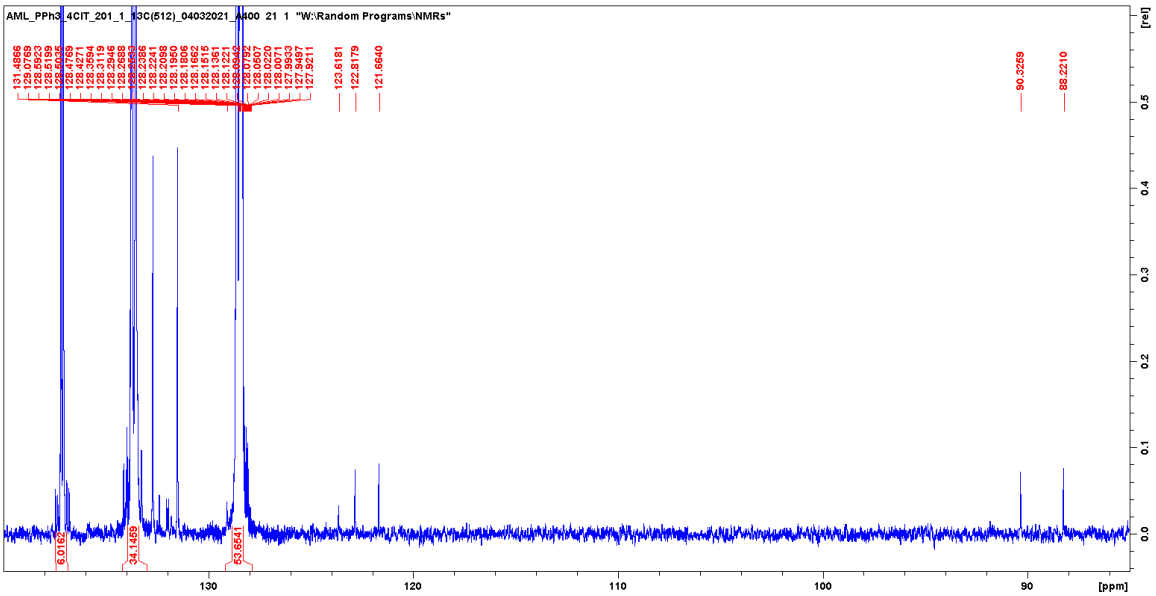

Figure 9.14: 20:1 PPh_3:4-ClT trial 1 spectrum.

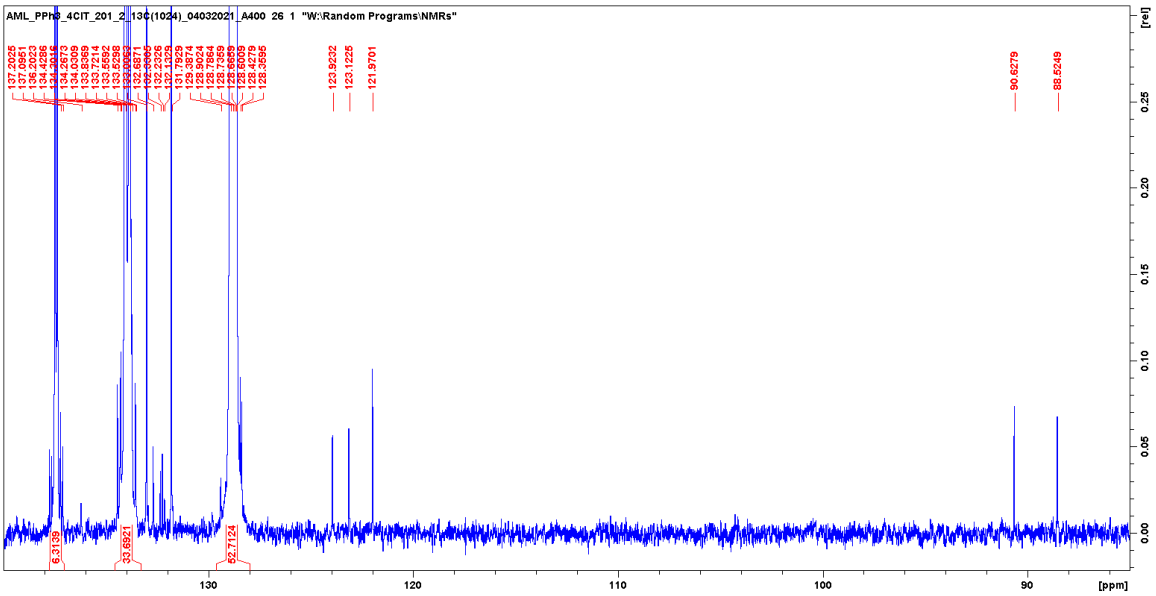

Figure 9.15: 20:1 PPh_3:4-ClT trial 2 spectrum.

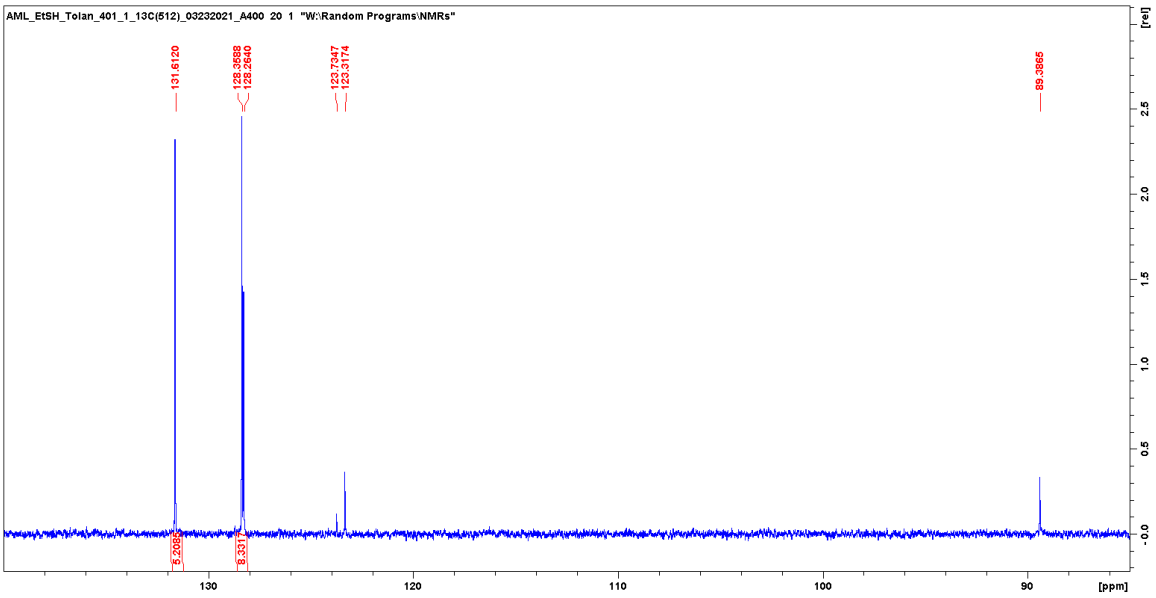

Figure 9.16: 40:1 EtSH:Tolan trial 1 spectrum.

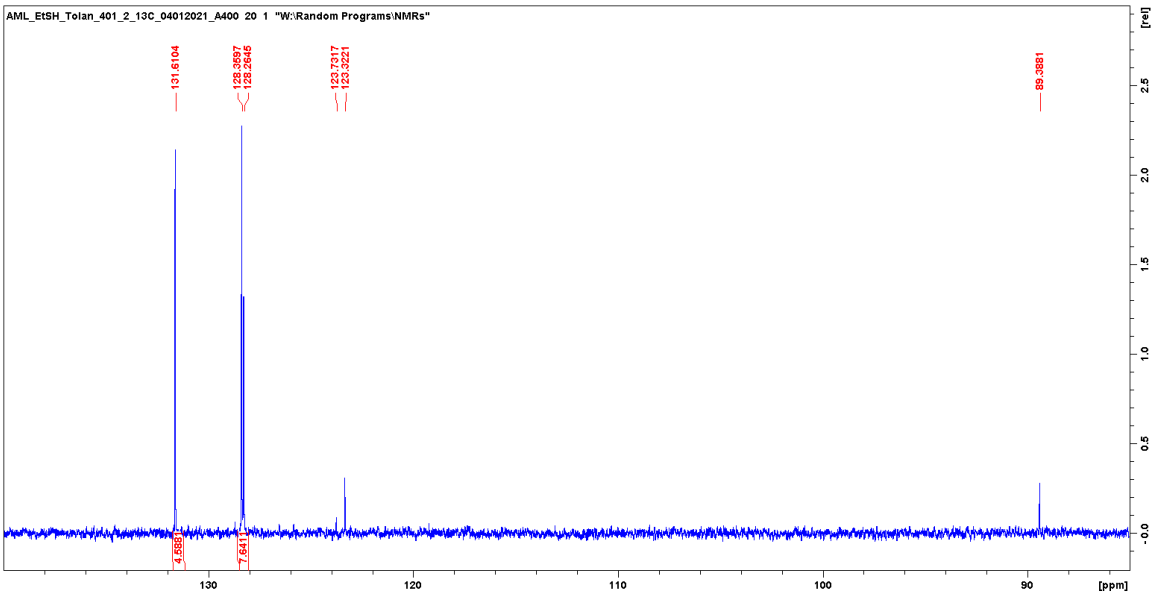

Figure 9.17: 40:1 EtSH:Tolan trial 2 spectrum.

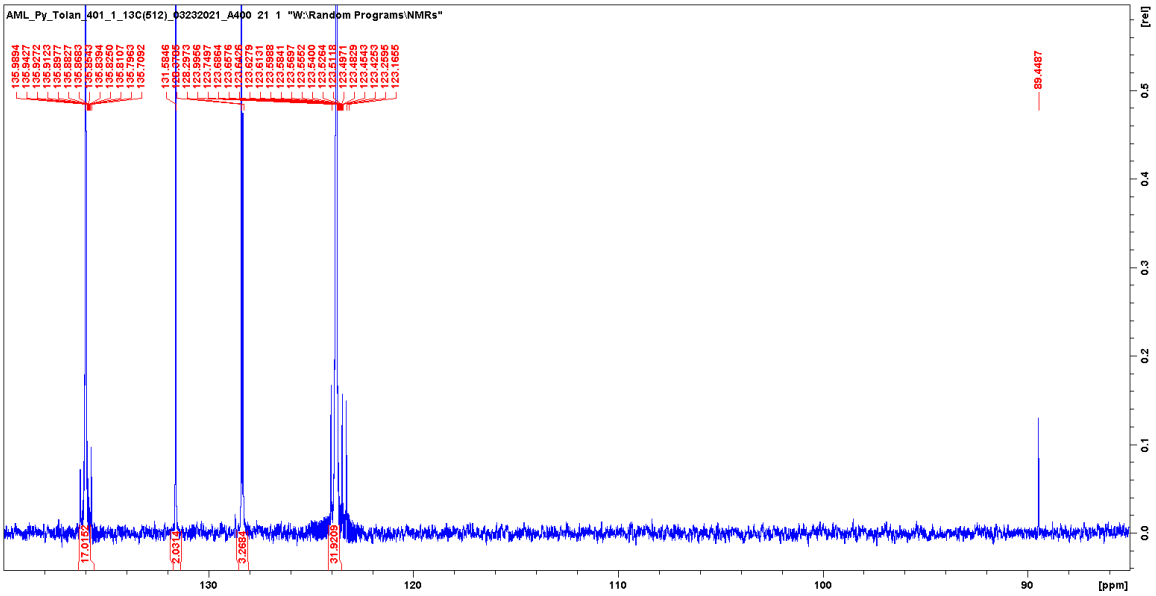

Figure 9.18: 40:1 Py:Tolan trial 1 spectrum.

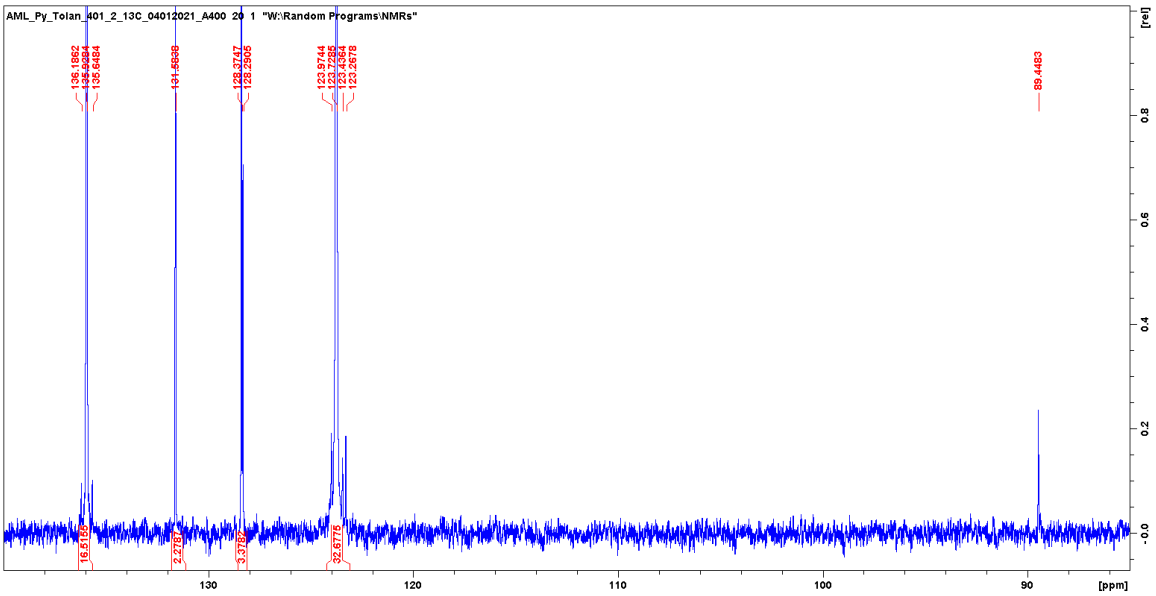

Figure 9.19: 40:1 Py:Tolan trial 2 spectrum.

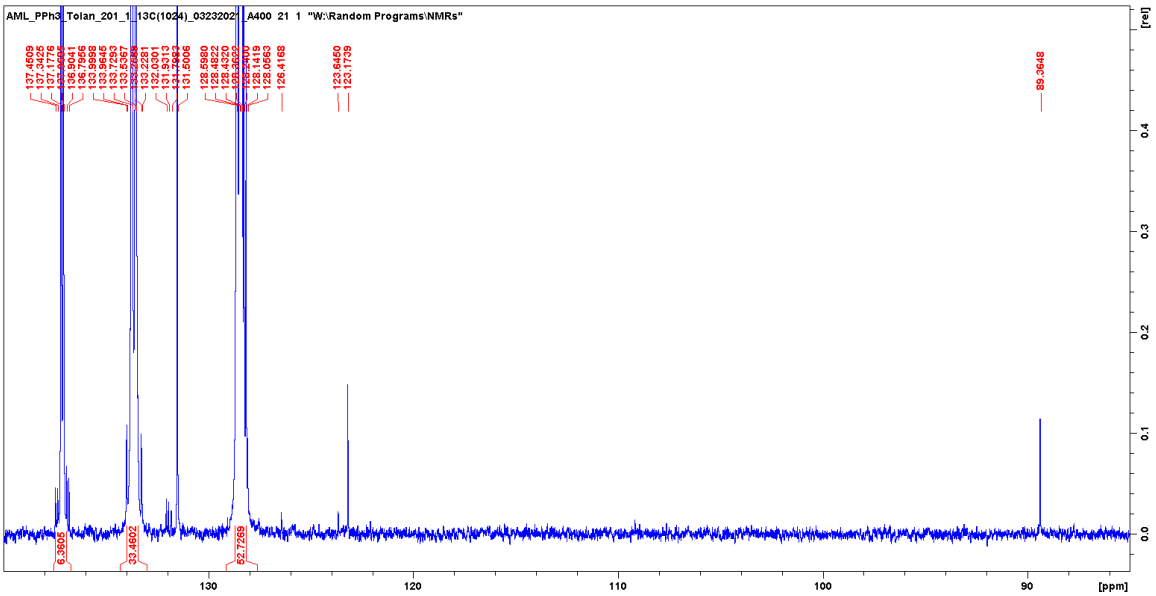

Figure 9.20: 20:1 PPh_3:Tolan trial 1 spectrum.

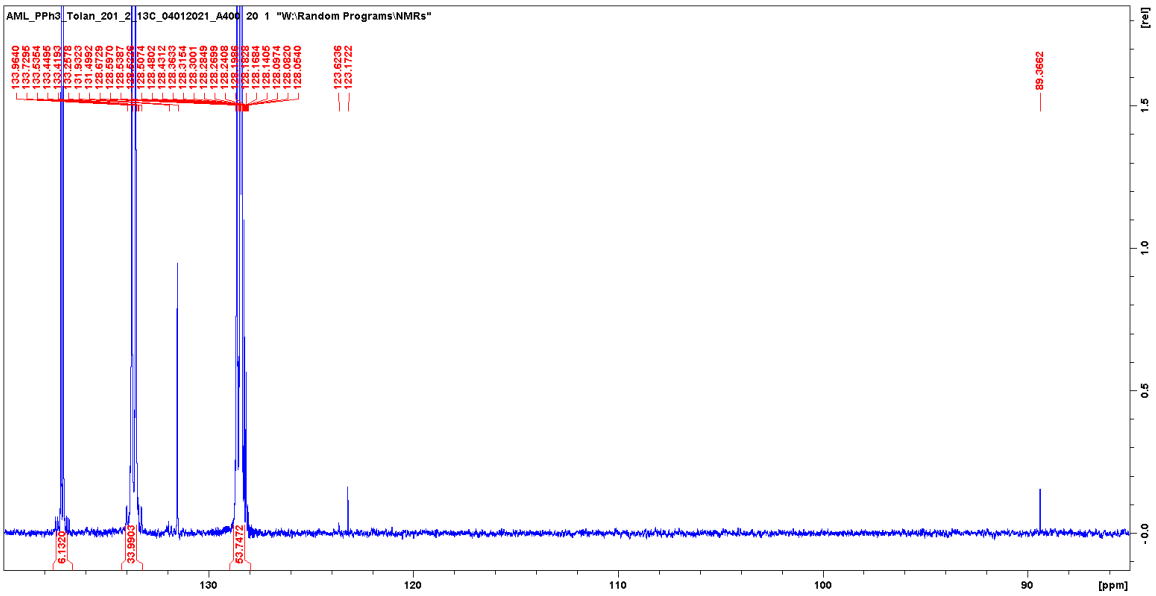

Figure 9.21: 20:1 PPh_3:Tolan trial 1 spectrum.

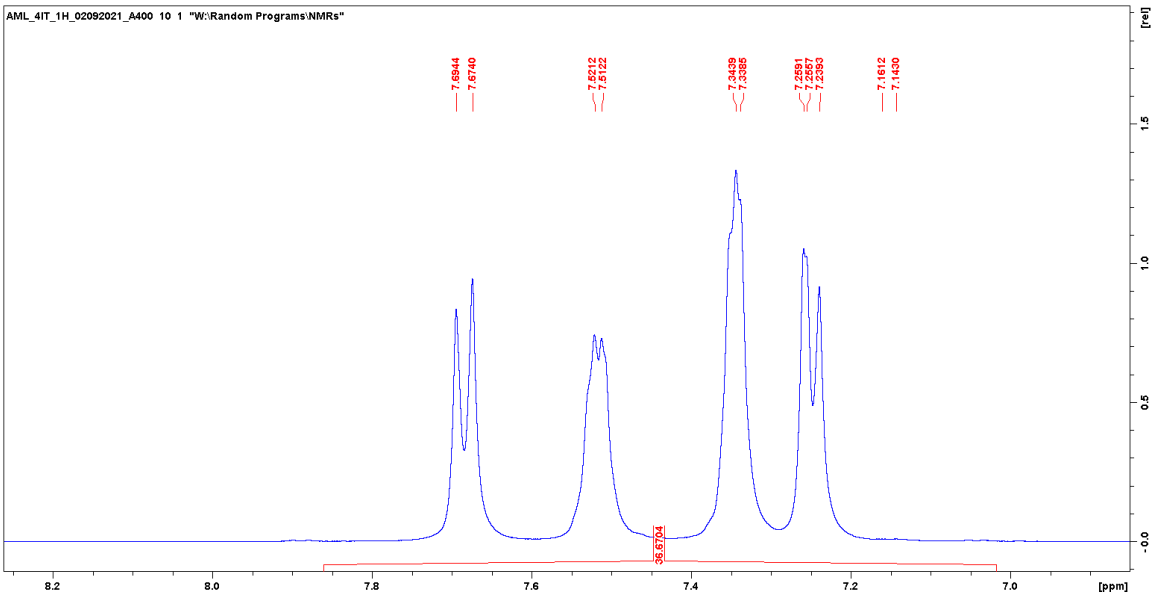

Figure 9.22: ^1H 4-IT spectrum.

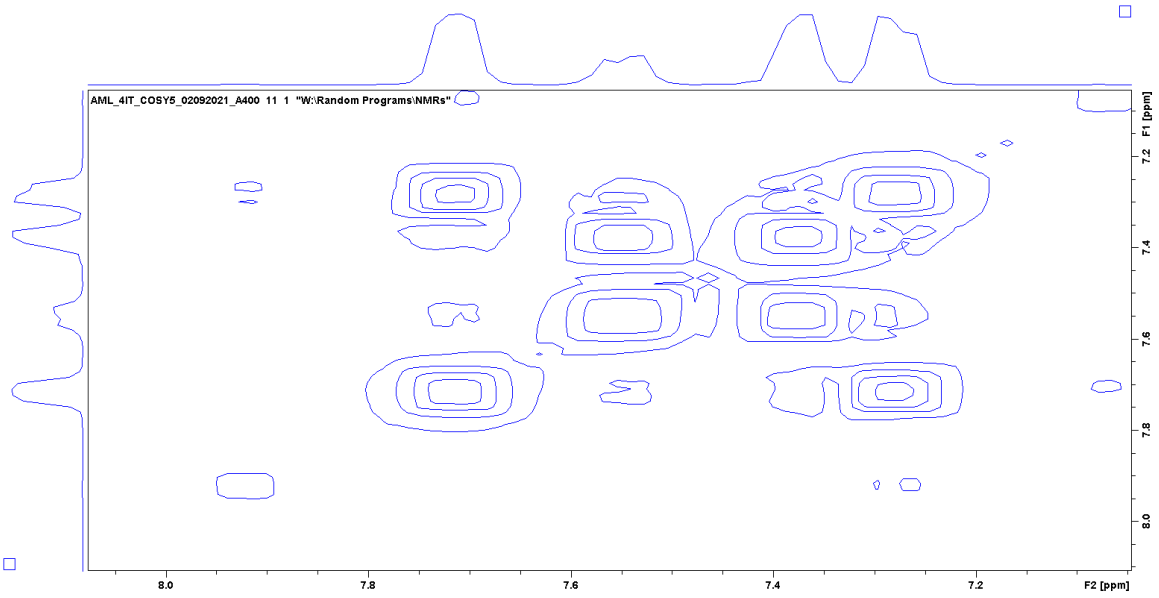

Figure 9.23: COSY 4-IT spectrum.

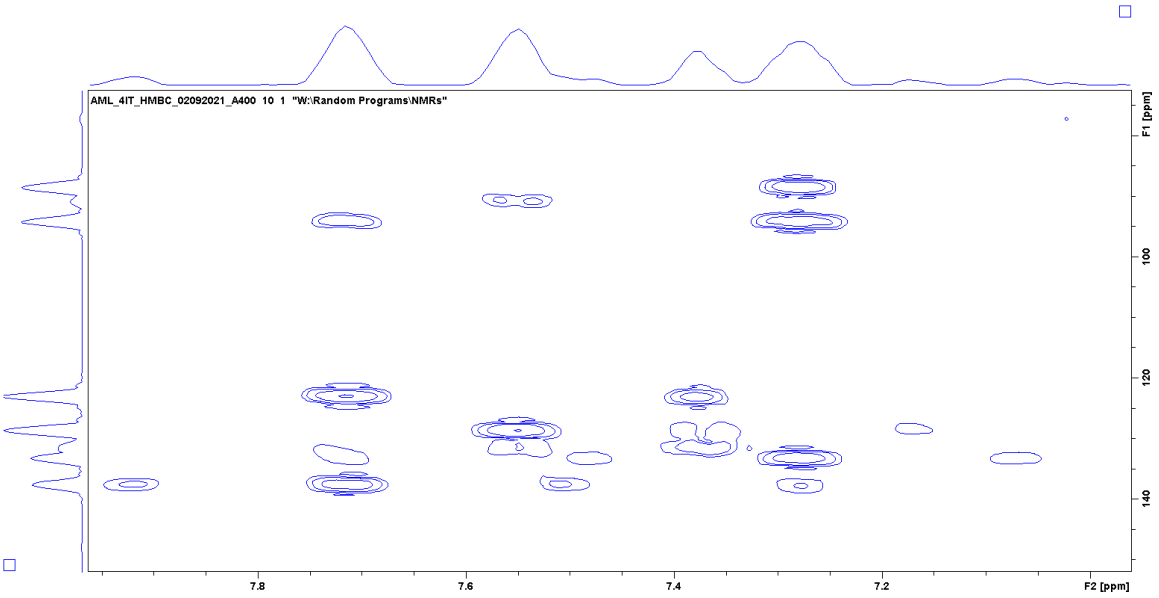

Figure 9.24 HMBC 4-IT spectrum

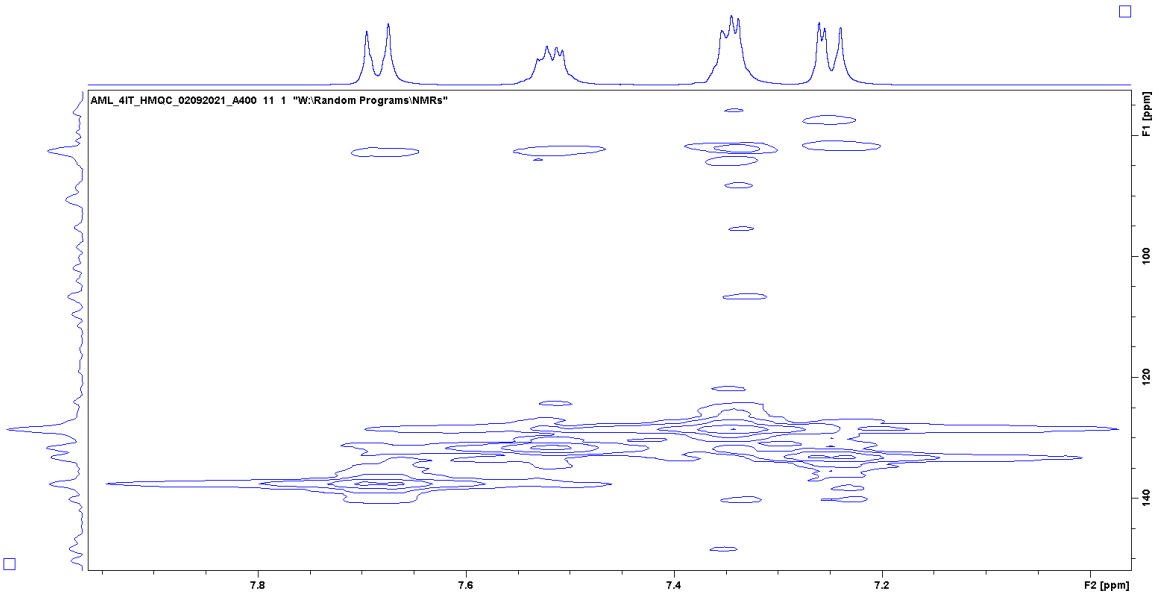

Figure 9.25: HMQC 4-IT spectrum.

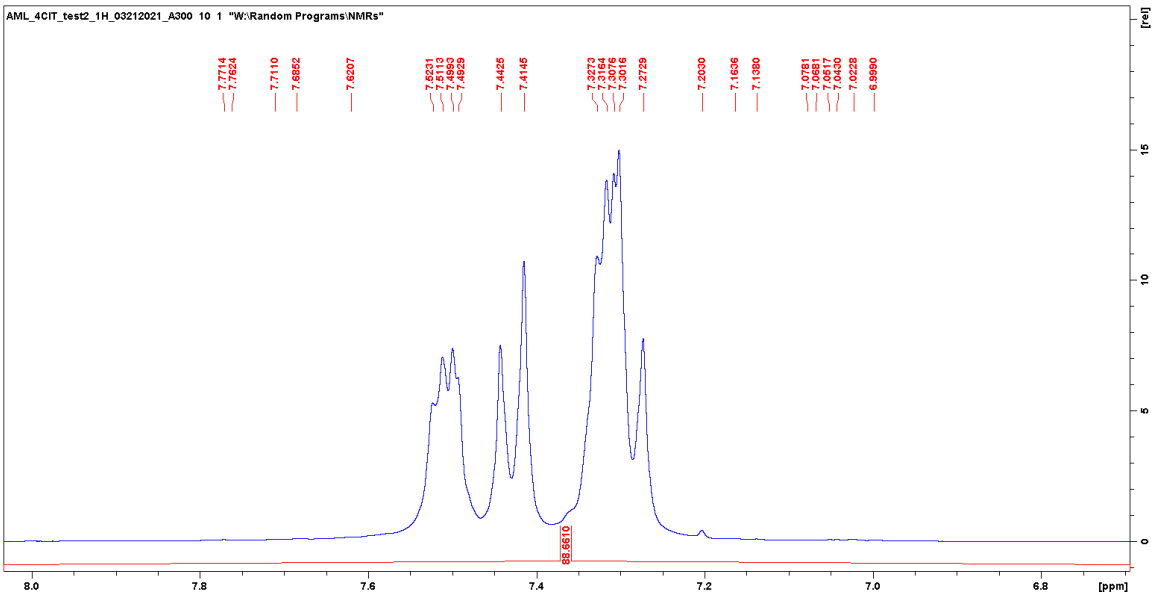

Figure 9.26: ^{1}H 4-ClT spectrum.

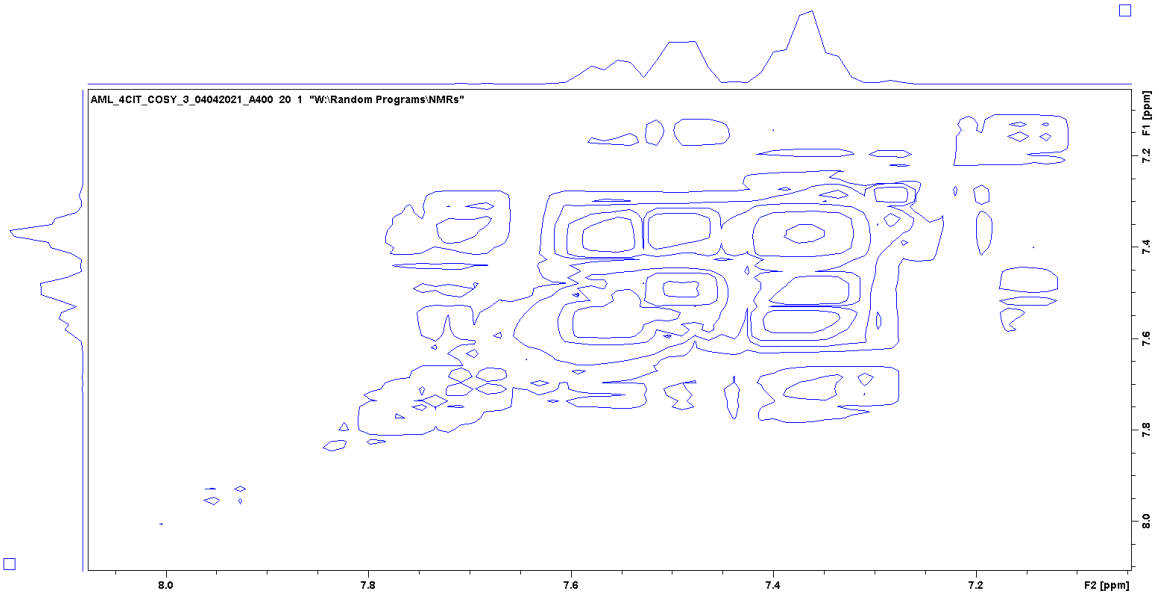

Figure 9.27: COSY 4-ClT spectrum.

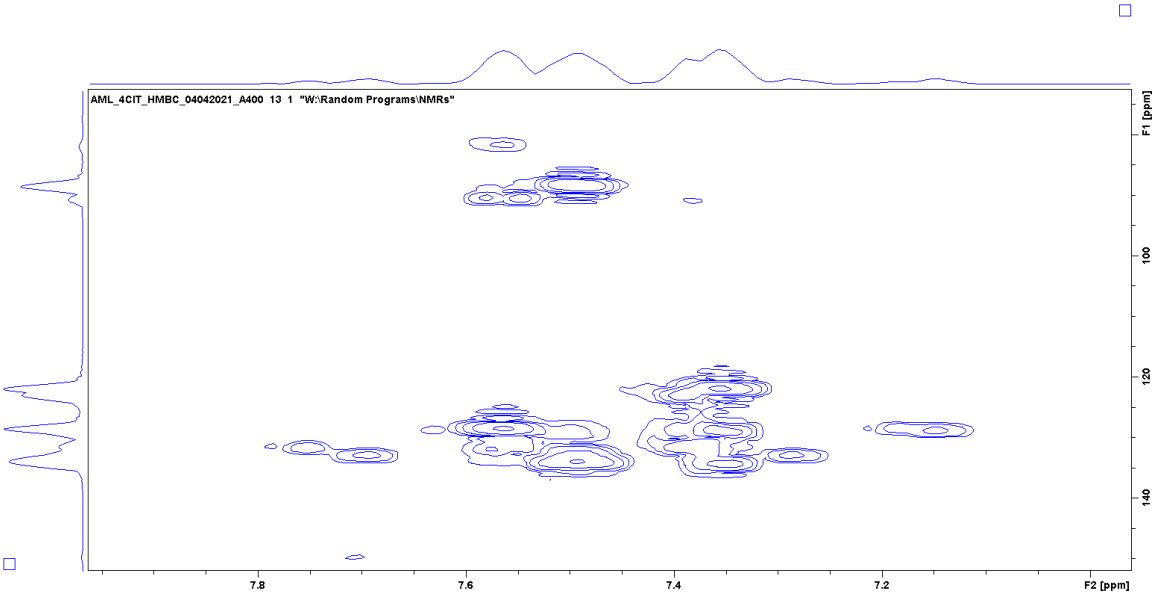

Figure 9.28: HMBC 4-ClT spectrum.

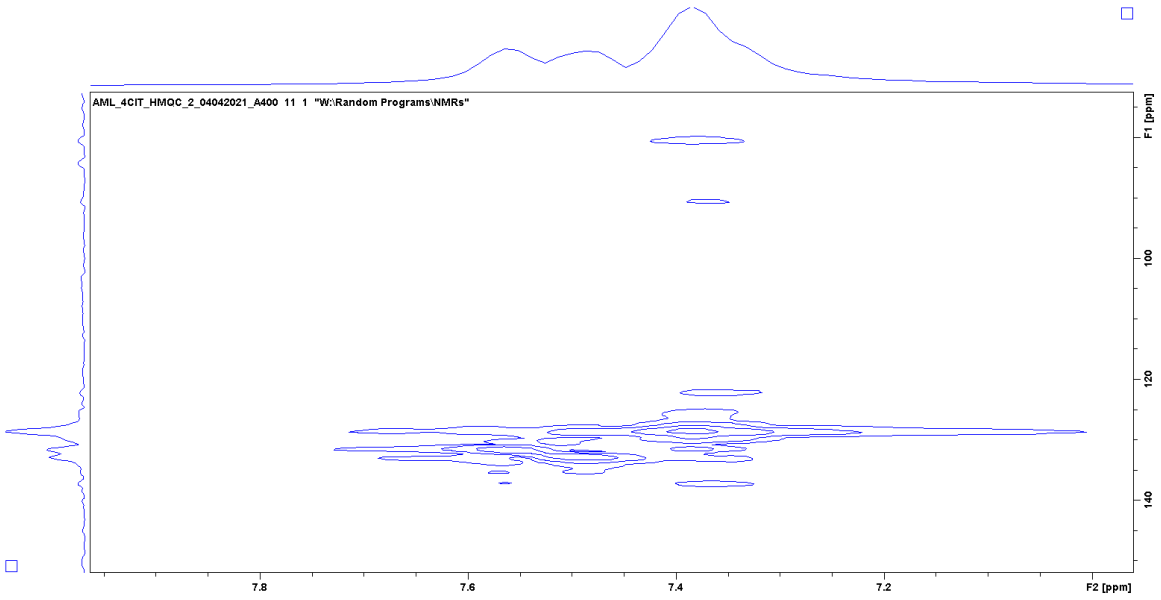

Figure 9.29: HMQC 4-ClT spectrum.